Dataset on Flood Risk Along the Niger River Upstream of Niamey

data

MDPI

Data Descriptor

Dataset on Flood Risk Along the Niger River Upstream of Niamey

Maurizio Tiepolo [1,*], Giorgio Cannella [2], Muhammad Abraiz [2], Ousmane Baoua [3], Elena Belcore [2], Daniele Ganora [2], Mohammed Ibrahim Housseini [4], Alejandro Marmolejo Gutierrez [2], Marco Piras [2], Francesco Saretto [2] and Riccardo Vesipa [2]

[1] Department of Regional & Urban Studies and Planning (DIST), Politecnico di Torino, Viale Pier Andrea Mattioli 39, 10125 Turin, Italy
[2] Department of Environment, Land and Infrastructure Engineering (DIATI), Politecnico di Torino, Corso Duca degli Abruzzi 24, 10129 Turin, Italy; giorgio.cannella@polito.it (G.C.); muhammad.abraiz@polito.it (M.A.); elena.belcore@polito.it (E.B.); daniele.ganora@polito.it (D.G.); alejandro.marmolejo@polito.it (A.M.G.); marco.piras@polito.it (M.P.); francesco.saretto@polito.it (F.S.); riccardo.vesipa@polito.it (R.V.)
[3] Direction de la Météorologie Nationale du Niger, 8 Rue du Grand Hôtel, Niamey BP 218, Niger; ousmanebaoua@yahoo.fr
[4] Ministère de l'Environnement, de l'Hydraulique et de l'Assainissement, Direction Générale des Ressources en Eau, Rond Point Hôpital de Niamey, Niamey BP 257, Niger; housseiniibrahimmohamed123@gmail.com
* Correspondence: maurizio.tiepolo@polito.it; Tel.: +39-011090749

Abstract

Knowledge of river flood risk in semiarid rural areas is often based on outdated, low-resolution geoinformation. Consequently, identification of exposed settlements, assets and risk-reduction measures remains challenging. This dataset provides up-to-date, fine-grained information for a rural area spanning 931 km^2 that is exposed to flooding from the Niger River and the Karma Wadi. The dataset includes information on (i) areas exposed to the two flood types that characterise the river's hydrological regime and flash floods from the wadi, (ii) flood-prone crops, buildings and (iii) measures for risk treatment. Discharge data, a 4 m horizontal-resolution digital elevation model, and two-dimensional hydraulic modelling with BASEMENT were used to identify flood-prone areas. Visual interpretation of high-resolution satellite imagery in Google Earth, together with field inspections, enabled the identification of exposed assets. The Information System on Rural Markets of Niger and house compensation values recognised during resettlement-related works enabled asset valuation. Risk was expressed in monetary terms as the product of flood probability and expected damage. Risk-reduction measures were identified with stakeholders through a SWOT analysis and prioritised using eight criteria. The dataset can support emergency plans, flood early warning systems, rescue and recovery operations and flood risk management.

Dataset: https://data.mendeley.com/datasets/9v349h653n/6 (accessed on 1 June 2026).

Keywords: early warning system; flood damage; flood exposure; hydraulic modelling; risk assessment; risk evaluation; risk management; risk reduction; risk treatment

Academic Editors: Yiding Bao and Qiang Wei

Received: 11 April 2026
Revised: 1 June 2026
Accepted: 6 June 2026
Published: 10 June 2026

1. Introduction

The increasing frequency and impact of river floods in Africa [1] call for open-access information to support flood risk management. The available open datasets mainly concern river discharge [2,3] and floodplain extension [4–6]. This information is released at the global or continental scale but rarely at the local scale [7–9]. Consequently, coarse altimetric and spatial resolution significantly affect risk estimation [10,11] and limit its use in flood prevention, preparedness, response and recovery. This lack of information is acute where large rivers cross densely populated or cultivated areas.

In Africa, the Niger River is the third-longest after the Nile and Congo Rivers (4167 km) and second only to the Congo River in discharge (7900 m^3/s). The 58 km stretch upstream of the city of Niamey (Niger) is among the most densely populated and cultivated areas along the river. However, over the past 15 years, catastrophic flooding has been more frequent in this stretch [12] (Figure 1).

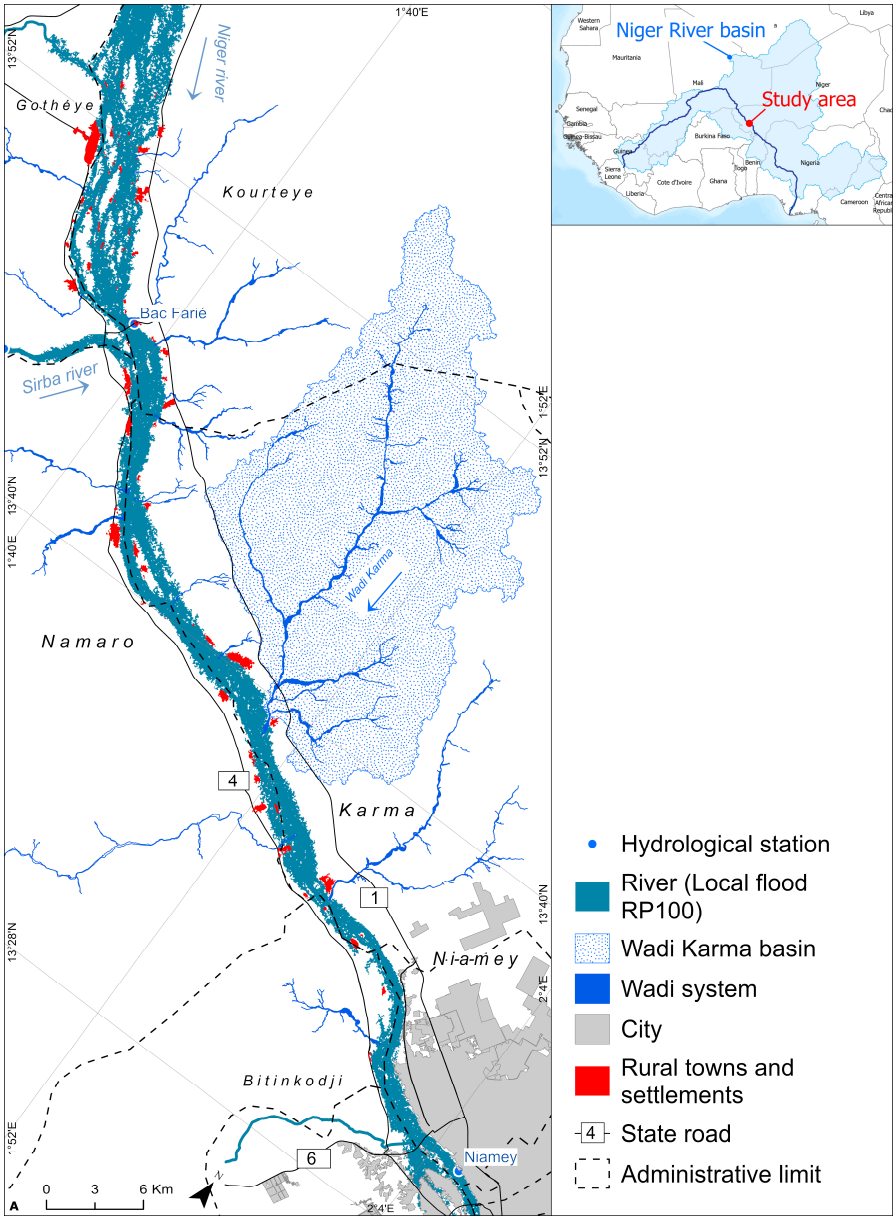

Figure 1. Stretch of the Niger River covered by the dataset. The study area consists of the flood-prone corridor along a 58 km reach of the Niger River upstream of Niamey, including the Karma Wadi basin.

To date, flood risk management along the Niger River has relied on three main sources of information. Rapid emergency mapping [13,14] identifies the floodplain near the peak of historic floods, but it captures only the main settlements and overlooks inundation depth and exposed assets. The Niger flood damage database [15] provides information on flooded assets by settlement since 1998. However, it does not localise individual buildings or fields, nor does it specify the flood triggering factor responsible for the damage (e.g., river inundation, flash flooding, or rainfall). More recently, Sentinel-2 images at flood peaks have been combined with asset visual interpretation from high-resolution satellite imagery and onsite inspections [16]. This approach, however, cannot account for flood magnitudes exceeding those observed to date. Accurate delineation of the inundation edge and depth for higher magnitude floods requires hydraulic modelling. The model is fed with the river discharge and the digital elevation model (DEM). However, the commonly used open-access Shuttle Radar Topography Mission (SRTM) DEM (2000, 30 m resolution) is inadequate for rivers with numerous channels, as in the study area, because it does not accurately present the current riverbank. Consequently, a higher-resolution DEM is required to model the Niger River floods.

Flood risk management also requires the identification of object-specific assets, which is rarely practised in rural areas of Low- to Medium-Income Countries (LMICs) [17,18].

The dataset includes river discharge probability, inundation extent and depth for return periods of 10, 30, and 100 years for the local and Guinean floods that characterise the river hydrology, exposed assets (buildings and crops), expected damage, priority risk-reduction measures, residual risk, and Cost–Benefit Analysis (CBA). In addition, the dataset includes hydrological information for the Karma Wadi basin, the main left-bank tributary of the river in the section under analysis. The basin covers approximately 382 km^2, with a maximum flow length of about 36 km, a form factor of 0.295, and an average terrain slope of approximately 17%. The data include the instantaneous unit hydrograph, the resulting flood hydrographs, land cover, and extension according to three elevation classes.

The dataset covers flood-prone areas along a 58 km stretch of the River Niger and the Wadi Karma basin, the largest tributary on the right bank, which causes damage to irrigated crops at its confluence with the river. Information is also provided by the administrative jurisdictions into which the study area is divided to support local prevention and recovery from flood damage.

The dataset was produced from Earth Observations (PlanetScope to generate the Digital Surface Model with 4 m of horizontal resolution, Google Earth to identify assets, Sentinel-2 to validate the flood zone), Niger River discharge and rainfall from stations, field inspections to validate exposed assets, agricultural statistics to estimate the value of assets, and discussions with riverside municipalities to identify risk treatment. The dataset was produced for the Flood Early Warning Local System in the Sahel (SLAPIS) project, which is developing an impact-based early warning system (EWS) along the Niger River and its main tributaries.

The public release of the dataset has five main benefits.

i. The dataset provides the baseline for monitoring assets exposed to floods with return periods (RPs) of 10, 30 and 100 years. The Civil Protection Agency (CPA), the Ministry of the Environment, Hydraulics and Sanitation (MEHS), the Authority of the Niger River Basin, the AGRHYMET regional centre, and researchers can reuse these data.
ii. Exposed assets organised by type, flood frequency, local jurisdiction and settlement enable the evolution of the flood EWS to an impact-based EWS [19,20]. They also support flood rescue and recovery operations and the preparation of local emergency plans. The data can be reused by the CPA, MEHS, five local governments along the

Niger River, the United Nations Office for the Coordination of Humanitarian Affairs, and scholars engaged in comparative studies in semiarid rural contexts.

iii. Maps show crops and buildings exposed to inundation depths less than 1 m, between 1 and 2 m and greater than 2 m. Local and regional governments can reuse these maps to support community flood-prevention efforts.

iv. Flood risk maps can be applied directly to zoning regulations in municipal plans (Plan de Sauvegarde, in French) and regional civil protection response organisation plans (Plan ORSEC, in French). Local and regional governments can reuse these maps directly.

v. Risk-reduction measures provide guidance for local governments and development partners aiming to reduce flood risk locally. This information can be directly reused by the relevant stakeholders.

2. Data Description

The dataset includes the inundation edge and depth (shapefiles and -PNG) for 10, 30 and 100-year RPs of local and Guinean floods, as well as a 100-year RP for Karma Wadi flash floods, exposed assets (spreadsheets and shapefiles), expected damage (spreadsheets) and risk-reduction measures (Figure 2, Table 1).

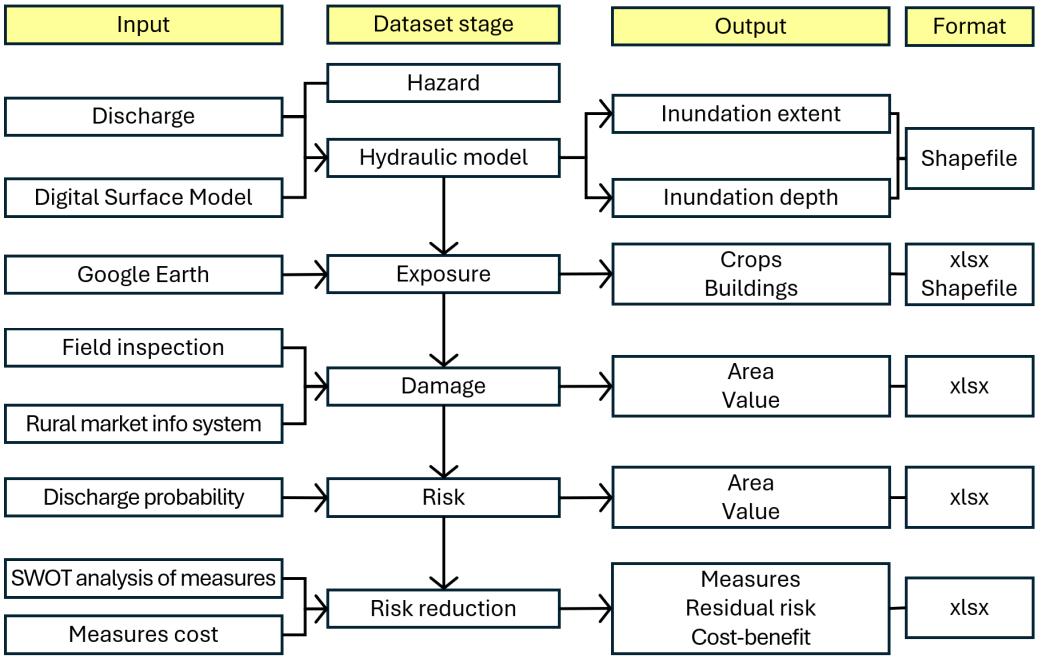

Figure 2. Workflow diagram.

2.1. Flood Risk Along the Niger River (Shapefiles)

All shape files included in the dataset use the same Coordinate Reference System (CRS), namely WGS 84/UTM Zone 31N (EPSG:32631), except for the flood-prone buildings layer, which is provided in the geographic coordinate system WGS 84 (EPSG:4326).

- *Flood-prone buildings* (zipped folder) contains shapefiles of buildings prone to flood events by return period, as identified from very high-resolution satellite images from February 2024, available in Google Earth Pro (GEP).
- *Flood-prone crops* (zipped folder) contains shapefiles of irrigated crops prone to flood events, identified by shape and texture from high-resolution GEP satellite images from February 2024 and verified through field inspections in February 2025.

- *Niger River flood edge* (zipped folder) contains shapefiles of areas prone to local and Guinean flooding at RP10, RP30 and RP100, resulting from two-dimensional (2D) hydraulic modelling with BASEMENT and a Digital Surface Model (DSM) at 4 m horizontal resolution.
- *Water depth* Guinean flood RP100 years (zipped folder) contains the inundation depth for Guinean flooding with RP100 years, which is derived from 2D BASEMENT hydraulic modelling.
- *Water depth* local flood RP100 (zipped folder) contains the inundation depth for local flooding with RP100 years, which is derived from 2D BASEMENT hydraulic modelling.

Table 1. List of shapefiles, spreadsheets and PNG files associated with the dataset titled "Flood Risk Along the Niger River Upstream of Niamey". The following Supporting Information can be downloaded at: https://data.mendeley.com/datasets/9v349h653n/6 (accessed on 1 June 2026).

Category	File or Table Names	Description
Flood risk assessment	Table S1	Fifty-five flood risk assessments in LMICs published since 2010 (.xlsx)
River discharge	Table S2	River discharge of local and Guinean floods with RP 10, 30 and 100 years
Karma Wadi	Table S3 Table S4	Hydrogram (.xlsx) Instantaneous unit hydrograph (.xlsx)
Inundation edge	Niger River flood edge.zip	Inundation edge by local and Guinean floods with RP10, 30 and 100 years
Inundation depth	Water depth Guinean flood RP 100.zip Water depth local flood RP 100.zip	Inundation depth of a Guinean flood RP100 (shapefiles) Inundation depth of a local flood RP100 (shapefiles)
Settlements	Figure 1S.png and Figure 2S.png	Flood-prone settlements (.PNG)
Assets	Flood-prone crops.zip Table S5 Flood-prone buildings.zip Table S6 Table S7 Table S8 Table S9	Crops (shapefiles) Crops (.xlsx) Buildings (shapefiles) Buildings (.xlsx) Crops by inundation depth (.xlsx) Building footprint by inundation depth Buildings number by inundation depth
Damage	Tables S10 and S11	Expected economic damage (.xlsx)
Risk	Table S12	Risk level (.xlsx)
Measures	Table S13 Table S14 Table S15	SWOT of potential measures (.xlsx) Priority measures (.xlsx) Karma Wadi area for water and soil conservation (WSC)(.xlsx)
Residual risk	Table S16	Residual risk by local and Guinean floods with RP 10 and 100 (.xlsx)
Cost–benefit	Table S17	Risk treatment CBA by local and Guinean floods RP10 and 100 years (.xlsx)

2.2. Flood Risk Along the Niger River (Spreadsheet)

Niger-FRA-Tables S1–S17 (.xlsx) contains 17 spreadsheets:

- *S1:* Seventy-eight flood risk assessments developed in rural LMICs since 2010.

- *S2:* River discharge by type and probability at three stations and one location on the Karma Wadi.
- *S3:* Karma Wadi hydrogram.
- *S4:* Instantaneous unit hydrographs at the hourly time scale for the Karma Wadi basin.
- *S5:* Sweet potato, pumpkins, pond rice, and horticulture in February 2024 prone to local and Guinean flooding assessed under each RP for local jurisdiction (Bitinkodji, Gotheye, Karma, Kourteye, Namaro).
- *S6:* Number and footprint (m^2) of buildings exposed to local and Guinean floods (RP10, RP30 and RP100), organised by settlement and local jurisdiction.
- *S7:* Sweet potato, pumpkins, traditional rice, horticulture that can be flooded at inundation depths < 1, 1–2 and >2 m according to local and Guinean floods with RP10, 30 and 100 years in Bitikondji. Gothèye, Karma, Kourteye and Namaro jurisdictions.
- *S8:* Footprint of buildings (m^2) that can be flooded at water depths < 1, 1–2 and >2 m by local and Guinean floods (RP10, RP30 and RP100), organised by local jurisdiction (Gothèye, Karma, Kourteye, Namaro).
- *S9:* Number of buildings that can be flooded at water depths < 1, 1–2 and >2 m by local and Guinean floods (RP10, RP30 and RP100), organised by local jurisdiction (Gothèye, Karma, Kourteye, Namaro).
- *S10:* Expected damage of local and Guinean floods RP10, RP30 and RP100, modelled with PlanetScope and SRTM DSMs.
- *S11:* Expected economic damage (EUR) to horticulture, pumpkins, traditional rice and sweet potato irrigated crops and buildings for Bitikondji, Gotheye, Karma, Kourteye and Namaro local jurisdictions.
- *S12:* Risk level for local and Guinean flood with 10, 30 and 100 years RP by Bitinkodji, Gothèye, Karma, Kourteye and Namaro local jurisdictions, expressed in Euros.
- *S13:* Strength–Weakness–Opportunities–Threats analysis conducted on 12 November 2025 with mayors, agricultural officers, water and sanitation officials, as well as AHA (Aménagement Hydro-Agricole) managers of Gothèye, Karma, Kourteye and Namaro.
- *S14:* Priority measures established with representatives of the four jurisdictions on 12 November 2025 using eight criteria.
- *S15:* Karma Wadi basin treated with trapezoidal bunds, half-moons and stone lines as of February 2024, area by altitude and map of altitude classes and sub-basins.
- *S16:* Residual risk by Guinean and local floods with RP10 and RP100 by Bitinkodji, Gothèye, Karma, Kourteye and Namaro local jurisdictions.
- *S17:* CBA of the risk treatments for local and Guinean floods (RP10 and RP100), and the benefit–cost ratio for AHA and settlements, by Bitinkodji, Gothèye, Karma, Kourteye and Namaro local jurisdictions.

2.3. Flood Risk Along the Niger River (PNG Files)

- *Figure 1S:* Flood-prone settlements between the Dargol–Niger and Sirba–Niger confluences, numbered sequentially as in Table S6.
- *Figure 2S:* Flood-prone settlements between the Sirba–Niger confluence and Niamey, numbered sequentially as in Table S6.

3. Methods

The dataset was produced in four stages: hazard assessment, damage estimation, risk analysis and risk evaluation. The hazard was determined through hydrological analysis. The damage was estimated using river discharge and RP combined with DSM in hydraulic modelling, and the value of the exposed assets. Risk analysis calculates the level of risk as the product of the flooding probability (1/RP), which is derived from the hydrological

analysis, and the expected damage. Risk evaluation incorporated risk-reduction measures informed by local knowledge and assessed the residual risk and the CBA.

3.1. Hydrological Analysis

The medium-Niger River crosses a hot, semiarid region, with a rainy season lasting from June to September. During this period, tributaries cause local flooding. Conversely, rainfall in the upper river, in Guinea and Mali, leads to the Guinean flood [12] during the dry season from November to February. The two flood peaks occur at completely different times of the hydrological year and never overlap. Over the last two decades, the local flood peaks at the Niamey gauge have exceeded the Guinean flood peaks in magnitude, reaching 2438 m^3/s compared to 2215 m^3/s in the 2024–2025 hydrological season.

Discharges for RP10, RP30, and RP100 years for the Niger River and its Sirba and Dargol tributaries were calculated using MEHS (Niger) data. These data were detrended and corrected [16], and the target RP discharges were estimated by fitting the generalised extreme value statistical model (Table S2). Owing to the limited data for the Dargol River, its target discharge values were derived by scaling those of the Sirba River.

Pluvial flooding in the Karma Wadi basin was analysed using daily rainfall data from the Karma station from the National Meteorological Directorate. RP30 and RP100 rainfall events were estimated using the metastatistical extreme-value distribution [21] to construct an hourly hyetograph using the Chicago method. The Horton method, which uses local parameters [22], was subsequently applied to calculate the net hyetograph. The resulting hydrograph was generated with the instantaneous unit hydrograph method (Table S2) implemented in a Geographic Information System (GIS) using a PlanetScope-derived DSM.

3.2. DSM Generation

A high-resolution (4 × 4 m) DSM was generated from PlanetScope daily, nearly global stereo imagery provided by the Planet Labs satellite constellation, with a spatial resolution of approximately 3 m and a ground sampling distance (GSD) of 3–4 m (Figure 3).

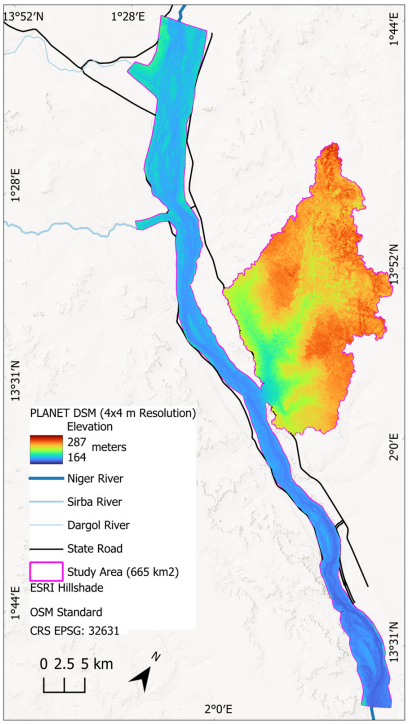

Figure 3. Digital Surface Model generated by high-resolution PlanetScope images over the Niger River and the Karma Wadi.

The DSM was generated using a bi-stereo matching workflow [23]. Owing to the scarcity of permanent global navigation satellite system stations near the study area, ground control points were extracted from the global SRTM DEM. These points were iteratively identified using map-to-image projections based on known geographic coordinates and elevations. The terrain features between the stereo images were automatically identified using hierarchical multiscale image matching in the Environment for Visualising Images (ENVI). Only the near-infrared band was used for image matching, as water bodies appear dark and are easily distinguishable. These tie points were subsequently used to establish epipolar geometry, align the conjugate points along a single axis, and generate the DSM. The DSM was georeferenced to the Universal Transverse Mercator 31N/WGS84 (EPSG:32631) projection, and all stereo-pair DSMs were mosaicked to produce a continuous elevation surface covering the entire study region.

3.3. Hydraulic Analysis

Hydraulic simulations were performed using the BASEMENT 2D hydraulic model. First, the computational domain was discretised into an unstructured triangular mesh, defined using breaklines, boundary-condition lines and the DSM. Breaklines delineated the computational domain and subdivided it into polygons with homogeneous roughness and a target element size. Boundary-condition lines identified model boundary segments where inflow or outflow were prescribed. The DSM was used to interpolate the bed elevation at the mesh nodes. Since a DSM was used instead of a Digital Terrain Model (DTM), the discharge correction technique proposed by Choné et al. [24] was applied to the Niger River simulations to account for the incomplete representation of the riverbed. For the Karma Wadi simulations, the DSM was produced during a dry period, when the ephemeral channels were not conveying water. Moreover, the semi-arid environment and low vegetation density make the DSM a suitable approximation of the terrain surface. After mesh generation, roughness values were assigned to each polygon, and the boundary conditions were specified. The model was then run for the three RP discharges of the local and Guinean floods of the Niger River, as well as for two RP discharges for the Karma Wadi basin. The resulting water depths were exported to Quantum GIS for visualisation and extraction of the flood extent (Niger River flood edge and water depth folders). The water-depth rasters were exported with a 4 m cell size, consistent with the spatial resolution of the DSM used for elevation interpolation, thereby avoiding an artificial increase in spatial precision beyond what is supported by the topographic input data.

3.4. Sensitivity Analysis

To assess the sensitivity of the hydraulic results to the vertical accuracy of the Planet DSM, a control analysis was conducted using auxiliary topographic data from previous research [25]. A drone DSM with 0.08 m horizontal resolution was produced for the Touré settlement, located along the Sirba River, approximately 34 km upstream of its confluence with the Niger River. The Sirba River is a major tributary of the Niger, and its lower reach lies in the same geomorphological and climatic setting as the Niger study area; furthermore, the same Planet DSM dataset covers both rivers. The Touré drone DSM captures a 1.8 km river reach, including the riverbed, and was therefore used as a high-resolution topographic benchmark against which the Planet DSM could be evaluated. Thirteen cross-sections were drawn along the control reach to compare the terrain elevations of the two DSMs (Figure 4).

Two representative cross-sections, Sections 4 and 8, were selected to illustrate the vertical comparison between the drone and Planet DSMs (Figure 5). Since both elevation datasets are Digital Surface Models (DSMs) rather than DTMs, local peaks may appear

in the profiles due to surface features such as trees or buildings. These features are more clearly captured by the high-resolution drone DSM.

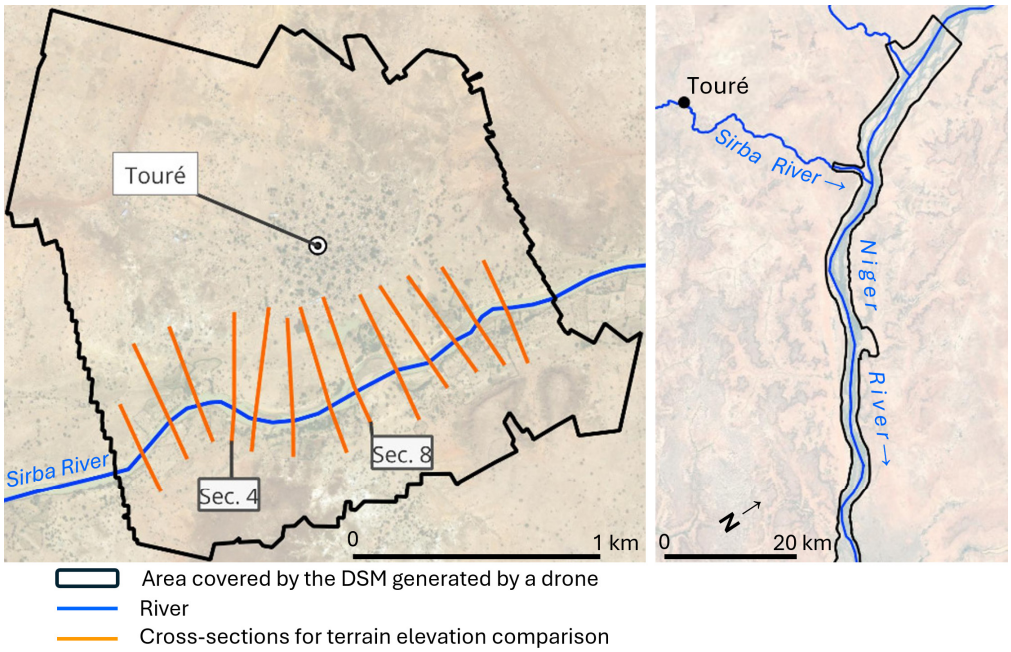

Figure 4. Cross-sections of the Sirba River in Touré, along which the DSM generated from PlanetScope imagery was compared with the DSM generated from drone imagery.

The drone and Planet DSMs were subsequently used as topographic inputs for 2D simulations of the control reach. Six discharges ranging from 500 to 1300 m^3/s were simulated to assess the sensitivity of the hydraulic results to the topographic input. The mean residual error decreased from 0.35 m at Q = 500 m^3/s to 0.14 m at Q = 1300 m^3/s, representing approximately 5% of the simulated water depths at design discharge. For reference, an independent roughness sensitivity test revealed that increasing Manning's n from 0.04 to 0.045 produced depth changes in the same order (0.25–0.45 m). The DSM-induced residual uncertainty is therefore comparable to the roughness uncertainty inherent to any 2D hydraulic model, confirming that the corrected Planet DSM does not introduce a disproportionate error into the flood simulations.

3.5. Expected Damage Analysis

Within the flood zones for each flood and RP, crops and buildings were identified by visually interpreting GEP imagery from February 2024. Fields were classified by shape and texture. Land inspections at 24 sites during the February 2025 flood verified crop types, resulting in five crop classes: AHA rice, traditional rice, horticultural crops, pumpkins, and sweet potatoes (Table S5). The surface area and number of assets exposed to inundation at each flood depth were subsequently calculated (Tables S6–S9). The benefits of using a higher-resolution DSM compared with the commonly used SRTM DEM were quantified in terms of the number of exposed locations and expected damage (Table S10).

Settlements were named according to the geographical coordinates reported in the national directory of localities (ReNaLoc) [26]. Three out of 43 settlements could not be located in the national directory and therefore remain unnamed.

The expected damage to crops and buildings was estimated using the agricultural market information system (SIMA) [27,28] and the compensation recognised for major works requiring resettlement [29] (Table S11). The peak stage of the local flood lasted one to two days, and the peak of the Guinean flood lasted more than a month. Crops that

remain submerged for such a long period of time, regardless of their stage of growth [30], are considered a total loss. Almost all the buildings are made of adobe. When adobe walls come into contact with water, even for a short time, they collapse, resulting in the complete loss of the structure.

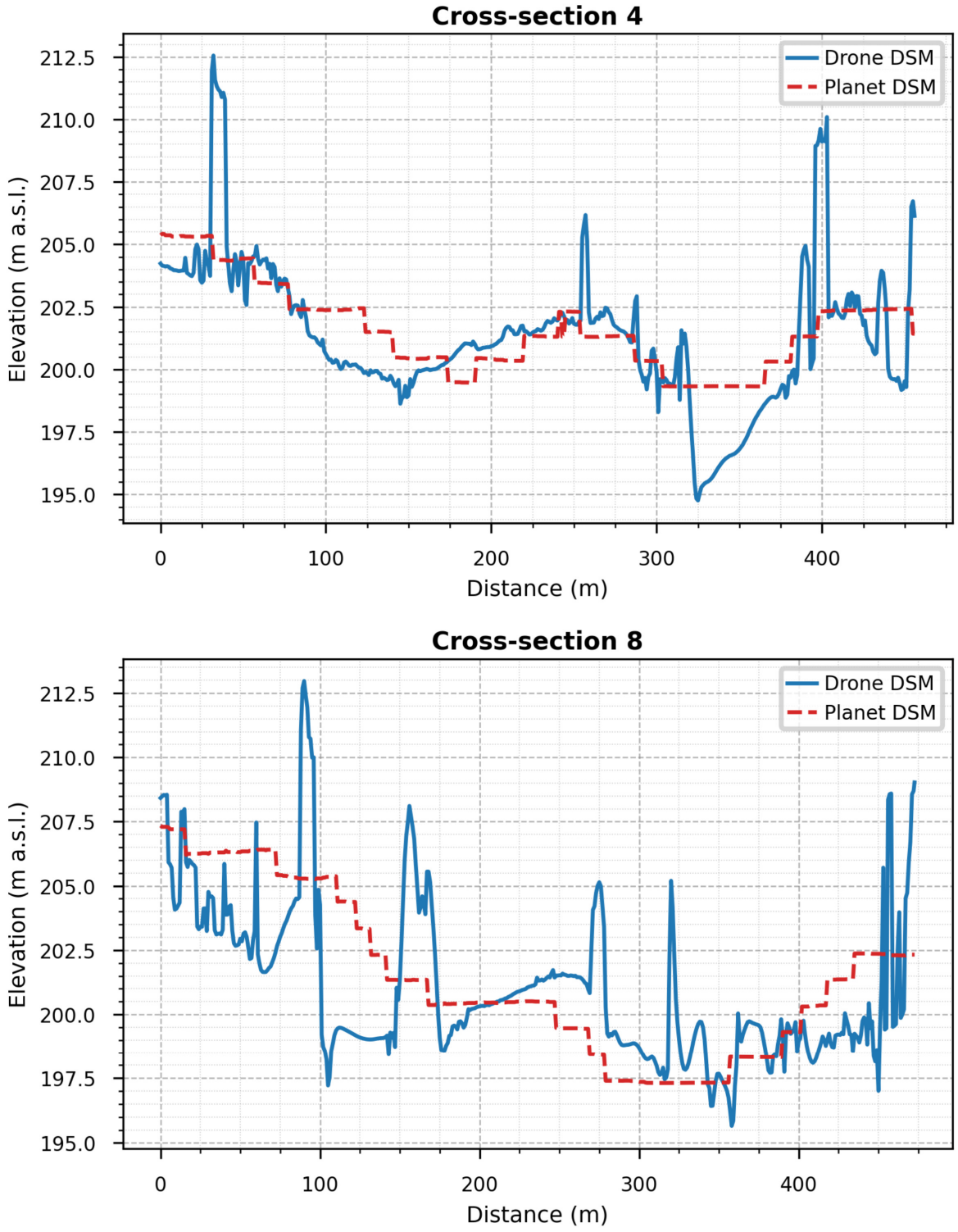

Figure 5. Elevation comparison of the drone and the PlanetScope DSMs on Sections 4 and 8 along the Sirba River in Touré.

3.6. Risk Analysis

The risk was calculated for each local government as the product of the hazard and the expected damage expressed in monetary terms [31–34] (Table S12).

3.7. Risk Evaluation

A SWOT analysis with stakeholders from four municipalities identified appropriate measures (Table S13), based on strategies commonly employed in semiarid areas [35,36], and prioritised them using eight criteria (Table S14).

Finally, based on the required quantity of measures (Table S15), residual risk (Table S16) and the benefit–cost ratio for risk reduction (Table S17) was calculated. The quantified benefits included annual per capita savings in healthcare expenses reported in the literature [37–39]. A 10-year horizon was adopted, reflecting the typical lifespan of the measures without maintenance, which was reduced to four years for half-moon structures [40]. Each measure was assumed to be implementable within one year. The net present value was calculated using the 5.5% legal discount rate established by the Central Bank of West African States for Niger [41]. A ratio greater than one indicates that the risk reduction is economically justified.

3.8. Validation

Flood edges were validated by overlaying the modelled flooded areas on 20 August 2024 and 16 February 2025, with those detected using the modified normalised difference water index applied to Sentinel-2 images. The flooded areas for these two datasets were generated using the BASEMENT 2D hydraulic model, with the corresponding river discharge entered for each date. The correspondence between the modelled and observed edges was quantified using the index $F = (Smod \cap Sobs)/(Smod \cup Sobs) \times 100$ [42], where Smod and Sobs denote the predicted and observed flooded areas, respectively. The index ranged from 55% to 68% across floods, substantially higher than the values obtained using the SRTM DEM for the same area and discharge rate with the same hydraulic model.

3.9. Limitations

Data scarcity poses a significant limitation to this work. Data from one basin (Sirba) were used as a proxy for another basin (Dargol). Although this approach can be justified using established methods, it increases the uncertainty of the results. Moreover, the hourly rainfall data were retrieved by theoretically downscaling the daily data, introducing additional uncertainties.

Although the DSM resolution is considerably higher than that typically used in semiarid rural areas, it remains lower than the 1 m resolution commonly applied in the Global North, which can only be achieved with expensive commercial DEMs. Producing DSMs at such high resolutions (<1 m) requires costly airborne campaigns and special flight permissions, which limit their feasibility along the Niger River. The dataset does not identify the few buildings constructed with durable materials.

4. User Notes

All shapefiles are raster-derived. The process used to generate the shapefiles and the semantic meaning of the geometries are specified in the metadata included in each layer. Shapefiles, .xlsx, and .PNG files can be linked to display settlements, buildings, and crops exposed to local and Guinean flooding, with RPs 10, 30, and 100 years depending on the depth of flooding (Figures 6–8).

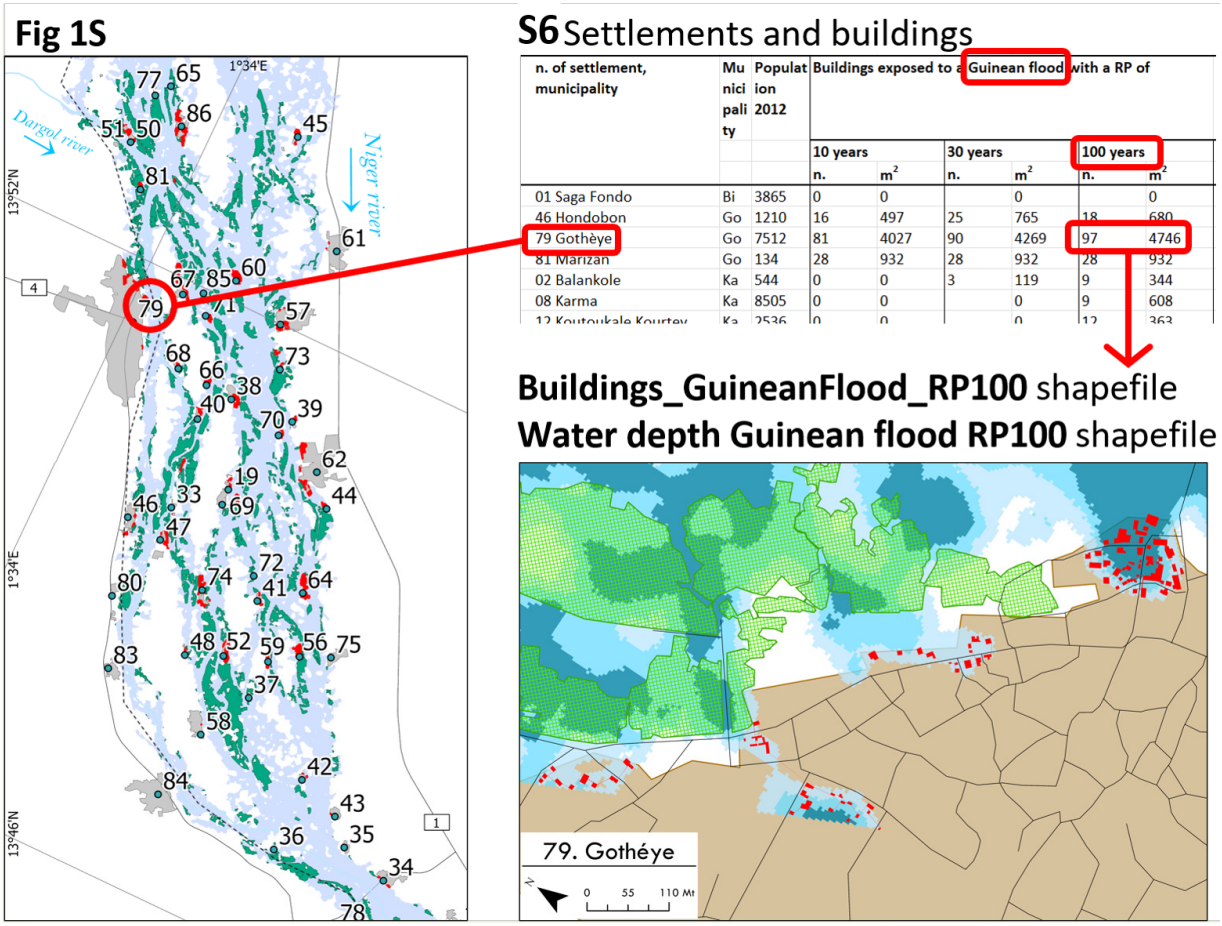

Figure 6. Link between flood-prone settlements and building data (.xlsx), their geographical location (PNG map) and the buildings exposed to water depth (shapefile).

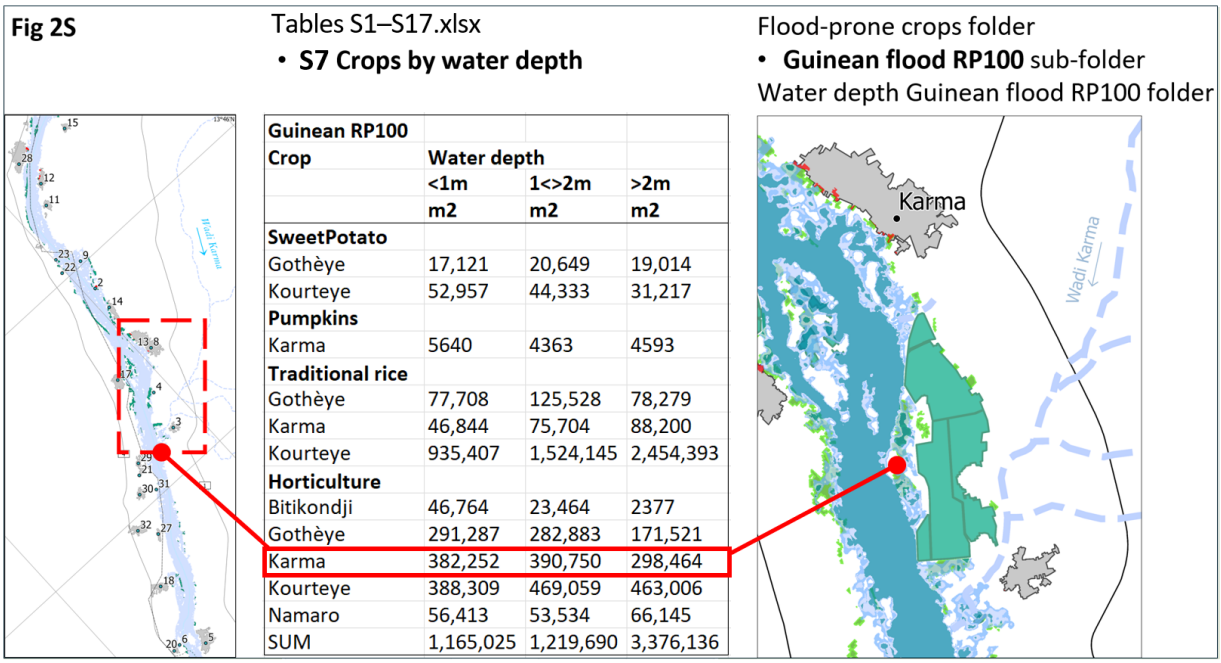

Figure 7. Link between flood-prone crops by water depth (XLS), their geographical location (PNG) and crops with associated water depth (shapefile).

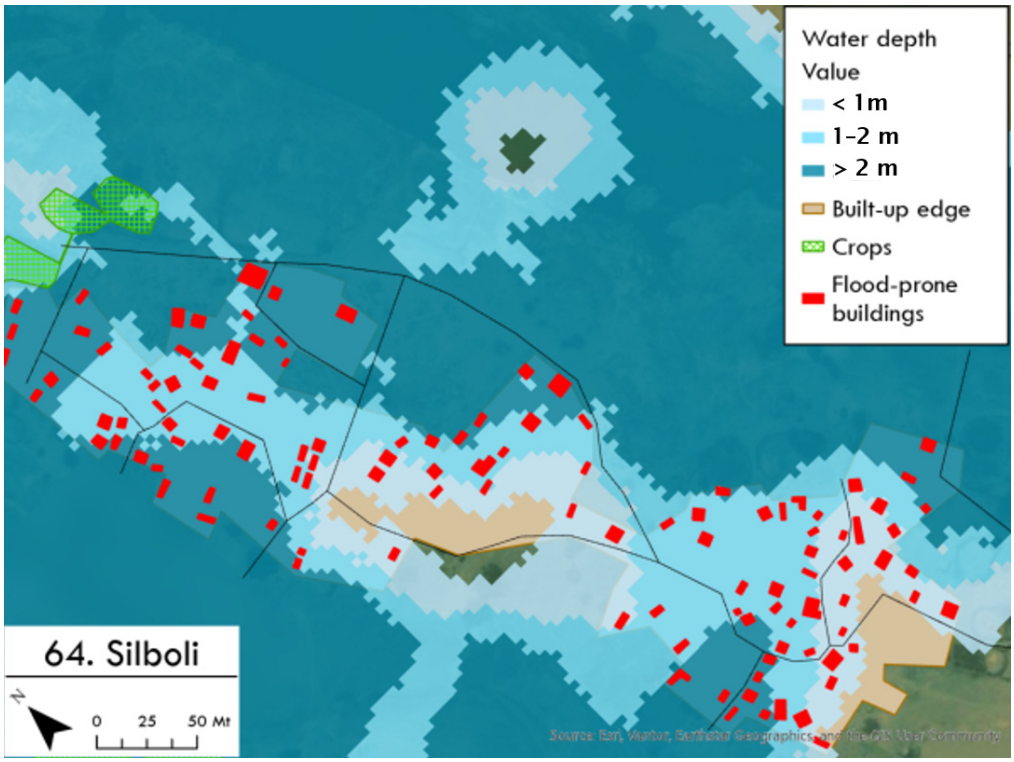

Figure 8. Map of buildings and fields at risk of flooding from the T100 Guinean flood, based on flood depth in the case of Silboli, municipality of Kourteye.

5. Conclusions

This paper presents a new dataset on flood risk along a 58 km stretch of the densely populated and cultivated Niger River, which is strategic for the food supply of the large city of Niamey. The exposed assets and expected damage from the three flood scenarios for each of the two flood types that characterise the hydrological regime of the Niger River provide a level of detail not previously available in datasets for LMICs. These results were obtained using a higher-resolution DSM than the conventional SRTM and ALOS PALSAR DEMs, photointerpretation of very high-resolution satellite imagery, and ground verification. The assessment of the modelled floodplain extension compared with that observed in Sentinel-2 images shows a coincidence of up to 68%, a value significantly higher than that achieved with the SRTM and ALOS PALSAR DEMs. The sensitivity of the DSM produced by the drone results in a vertical average error of the floodplain of 0.14–0.35 m, depending on the river discharge (500–1300 m^3/s). This dataset, with respect to the floods, can contribute to prevention, preparedness, response and recovery along the Niger River. It can enable the construction of an impact-based flood EWS. More generally, this dataset can be extended to other sections of the Niger River and along the tributaries that cause the most flood damage, such as the Sirba River.

Supplementary Materials: The following supporting information can be downloaded at: https://data.mendeley.com/datasets/9v349h653n/6 (accessed on 1 June 2026), Tables S1–S17, Figures 1S and 2S.

Author Contributions: Conceptualisation, D.G., M.P., M.T. and R.V.; methodology, E.B., D.G., M.P., M.T. and R.V.; software, M.A. and R.V.; validation, G.C.; formal analysis, A.M.G. and F.S.; investigation, M.A., G.C., O.B., A.M.G., F.S. and M.T.; resources, M.P. and R.V.; data curation, M.I.H.; writing—original draft preparation, M.A., A.M.G., F.S. and M.T.; writing—review and editing R.V.; visualisation, M.A., G.C. and A.M.G.; supervision, M.T.; project administration, M.T.; funding acquisition, M.T. All authors have read and agreed to the published version of the manuscript.

Funding: This research was funded by the Italian Agency for Development Cooperation, grant AID 012487.

Institutional Review Board Statement: Not applicable.

Informed Consent Statement: Not applicable.

Data Availability Statement: The data presented in this article are available at https://data.mendeley.com/datasets/9v349h653n/6 (access on 1 June 2026).

Acknowledgments: The authors thank Gaptia Lawan Katiellou (Direction de la Météorologie Nationale du Niger), Moumouni Hassane (agriculture Gothèye), Hamadou Ali (agriculture Kourteye), Abdoul Kader Seyni (agriculture Karma), Boubacar Abdou (agriculture Namaro) and Abdoul Samadou Souley Issa (AHA Koutoukalé). The authors have reviewed and edited the output and take full responsibility for the content of this publication.

Conflicts of Interest: The authors declare no conflicts of interest. The Italian Agency for Development Cooperation had no role in the design of the study, in the collection, analysis, or interpretation of data, in the writing of the manuscript, or in the decision to publish the results.

Abbreviations

The following abbreviations are used in this manuscript:

AGRHYMET	Centre Regional de Formation et d'Application en Agrométéorologie et Hydrologie Opérationnelle
AHA	Aménagement Hydro Agricole
CBA	Cost–Benefit Analysis
CPA	Civil Protection Agency
DEM	Digital Elevation Model
DSM	Digital Surface Model
ENVI	Environment for Visualising Images
EUR	Euro
EWS	Early Warning System
GEP	Google Earth Pro
GIS	Geographic Information System
LMICs	Low- Middle-income Countries
MEHS	Ministry of the Environment, Hydraulics and Sanitation
ORSEC	Organisation des Secours
PNG	Portable Network Graphic
ReNaLoc	Répertoire National des Localités
RP	Return Period
RPC	Rational Polynomial Coefficient
SIMA	Système d'Information sur les Marchés Agricoles
SRTM	Shuttle Radar Topography Mission
SWOT	Strengths–Weaknesses–Opportunities–Threats
2D	Two Dimensional
WSC	Water and Soil Conservation

References

1. Houteta, D.K.; Sylla, M.B.; Tall, M.; Dajuma, A.; Pal, J.S.; Lennard, C.; Wolski, P.; Moufouma-Okia, W.; Hewitson, B. Spatial and Temporal Trend Analysis of Flood Events Across Africa During the Historical Period. *Water* **2025**, *17*, 3531. [CrossRef]
2. Harrigan, S.; Zsoter, E.; Alfieri, L.; Prudhomme, C.; Salamon, P.; Wetterhall, F.; Barnard, C.; Cloke, H.; Pappenberger, F. GloFAS-ERA5 operational global river discharge reanalysis 1979–present. *Earth Syst. Sci. Data* **2020**, *12*, 2043–2060. [CrossRef]
3. Tramblay, Y.; Rouché, N.; Paturel, J.-E.; Mahé, G.; Boyer, J.-F.; Amoussou, E.; Bodian, A.; Dacosta, H.; Dakhlaoui, H.; Dezetter, A.; et al. ADHI: The African database of hydrometric indices (1950–2018). *Earth Syst. Sci. Data* **2021**, *13*, 1547–1560. [CrossRef]
4. Nardi, F.; Annis, A.; Di Baldassarre, G.; Vivoni, E.R.; Grimaldi, S. GFPLAIN250m,a global high-resolution datasetof Earth's floodplains. *Sci. Data* **2018**, *6*, 180309. [CrossRef]

5. Rajib, A.; Zheng, Q.; Lane, C.R.; Golden, H.E.; Christensen, J.R.; Isibor, I.I.; Johnson, K. Human alterations of the global floodplains 1992–2019. *Sci. Data* **2023**, *10*, 499. [CrossRef]
6. Miura, Y.; Shamsudduha, M.; Suppasri, A.; Sano, D. A global multi-sensor dataset of surface water indices from Landsat-8 and Sentinel-2 satellite measurements. *Sci. Data* **2025**, *12*, 1253. [CrossRef] [PubMed]
7. Ogarekpe, N.; Obio, E.; Tenebe, I.; Emenike, P.G.; Nnaji, C. A dataset for the flood vulnerability assessment of the upper Cross River basin using morphometric analysis. *Data Brief* **2020**, *30*, 105344. [CrossRef] [PubMed]
8. Mdegla, L.; De Bock, Y.; Luhanga, E.; Leo, J.; Mannens, E. Monitoring Kikuletwa river levels in northern Tanzania: A data set unlocking insights for effective flood early warning systems. *Data Brief* **2023**, *49*, 109395. [CrossRef]
9. Akopti, K.; Velpuri, N.M.; Mizukami, N.; Kagone, S.; Leh, M.; Mekonnen, K.; Owusu, A.; Tinonetsana, P.; Phiri, M.; Madushanka, L.; et al. Advancing water security in Africa with new high-resolution discharge data. *Sci. Data* **2024**, *11*, 1195. [CrossRef]
10. Gosset, P.; Dibi-Anoh, A.; Schumann, G.; Hostache, R.; Paris, A.; Zahiri, E.P.; Kacou, M.; Gal, L. Hydrometeorological extreme events in Africa: The role of satellite observations for monitoring pluvial and fluvial flood risk. *Surv. Geophys.* **2023**, *44*, 197–223. [CrossRef]
11. Komolafe, A.A.; Herath, S.; Avtar, R. Sensitivity of flood damage estimation to spatial resolution. *J. Flood Risk Manag.* **2018**, *11*, S370–S381. [CrossRef]
12. Massazza, G.; Bacci, M.; Descroix, L.; Ibrahim, M.H.; Fiorillo, E.; Katiellou, G.L.; Panthou, G.; Pezzoli, A.; Rosso, M.; Sauzedde, E.; et al. Recent Changes in Hydroclimatic Patterns over Medium Niger River Basins at the Origin of the 2020 Flood in Niamey (Niger). *Water* **2021**, *13*, 1659. [CrossRef]
13. Service Régional de Traitement D'image et de Télédétection. Niger-Tillaberi. Flood Extent Map—Detail Observation the 09/09/2012. 2012. Available online: https://sertit.unistra.fr/en/rapid-mapping/cartoproduct/45/#group (accessed on 22 November 2025).
14. Copernicus Emergency Management Service. Tillaberi-Niger Flood-Situation as of 10/09/2017 Delineation Map. 2017. Available online: https://cems-mapping-website.s3.eu-west-1.amazonaws.com/static/activations/EMSR235/EMSR235_03TILLABERI_0-1DELINEATION_MAP_v1_200dpi.pdf (accessed on 22 November 2025).
15. Fiorillo, E.; Crisci, A.; Issa, H.; Maracchi, G.; Morabito, M.; Tarchiani, V. Recent changes of floods and related impacts in Niger based on the ANADIA Niger flood database. *Climate* **2018**, *6*, 59. [CrossRef]
16. Tiepolo, M.; Abraiz, M.; Bacci, M.; Baoua, O.; Belcore, E.; Cannella, G.; Fiorillo, E.; Ganora, G.; Housseini, I.M.; Katiellou, G.L.; et al. Flood damage risk mapping along the River Niger: Ten benefits of a participated approach. *Climate* **2025**, *13*, 80. [CrossRef]
17. Najafi, H.; Shrestha, P.K.; Rakovec, O.; Apel, H.; Vorogushyn, S.; Kumar, R.; Thober, S.; Merz, B.; Samaniego, L. High-resolution impact-based early warning system for riverine flooding. *Nat. Commun.* **2023**, *15*, 3726. [CrossRef]
18. Glas, H.; De Maeyer, P.; Merisier, S.; Deruyter, G. Development of a low-cost methodology for data acquisition and flood risk assessment in the floodplain of the river Moustiques in Haiti. *J. Flood Risk Manag.* **2020**, *13*, e12608. [CrossRef]
19. Diani, K.; Hamza, M.H.; Elbelrhiti, H.; Kacimi, I.; Faqihi, F.Z.; Haghighi, A.T.; El Amrani, M.; Hahou, Y.; Masmoudi, L.; Lahcen, O.; et al. Flood risk assessment, a case study in an arid environment of Southeast Morocco. *Open Geosci.* **2024**, *16*, 20220607. [CrossRef]
20. Tarchiani, V.; Massazza, G.; Rosso, M.; Tiepolo, M.; Pezzoli, A.; Housseini Ibrahim, M.; Katiellou, G.L.; Tamagnone, P.; De Filippis, T.; Rocchi, L. Community and impact based early warning system for flood risk preparedness: The experience of the Sirba River in Niger. *Sustainability* **2020**, *12*, 1802. [CrossRef]
21. Marani, M.; Ignaccolo, M. A metastatistical approach to rainfall extremes. *Adv. Water Resour.* **2015**, *79*, 121–126. [CrossRef]
22. Nguyen, V.T.; Georges, D.; Besançon, G. Application of variational calculus to parameter estimation in a real hydrological system. *Eur. J. Control* **2021**, *60*, 11–19. [CrossRef]
23. Abraiz, M.; Belcore, E.; Piras, M. DEM generation from multi-view satellite images in Sub-Sahel region. *Int. Arch. Photogramm. Remote Sens. Spat. Inf. Sci.* **2025**, *XLVIII-M-6-2025*, 9–14. [CrossRef]
24. Choné, G.; Biron, P.M.; Buffin-Bélanger, T. Flood hazard mapping techniques with LiDAR in the absence of river bathymetry data. *E3S Web Conf.* **2018**, *40*, 06005. [CrossRef]
25. Belcore, E.; Piras, M.; Pezzoli, A.; Massazza, G.; Rosso, M. Raspberry PI 3 multispectral low-cost sensor for UAV based remote sensing. Case study in South-west Niger. *Int. Arch. Photogramm. Remote Sens. Spat. Inf. Sci.* **2019**, *XLII-2/W13*, 207–214. [CrossRef]
26. République du Niger, Institut National de la Statistique. *Répertoire National des Localités (ReNaLoc)*; INS: Niamey, Niger, 2014. Available online: https://www.stat-niger.org/wp-content/uploads/renaloc/ReNaLoc_RGPH_2012.pdf (accessed on 9 June 2025).
27. République du Niger, Ministère du Commerce et de l'Industrie. SIMA. *Bull. Hebdo Céréales* **2025**, *786*, 1. Available online: https://simaniger.net/download/bulletin-hebdo-cereales-n786-semaine-n8-du-mercredi-19-au-mardi-25-fevrier-202525/ (accessed on 8 July 2025).

28. République du Niger, Ministère du Commerce et de l'Industrie. SIMA. *Bull. Hebdo. Fruits Legumes* **2025**, *633*. Available online: https://simaniger.net/download/bulletin-mensuel-des-produits-agricoles-n333-du-mois-de-fevrier-2025/ (accessed on 8 July 2025).
29. République du Niger, Ministère des Transports et de l'Équipement. *Plan D'actions de Réinstallation (PAR) du Tronçon Diffa-N'guigmi sur Environ 35 Kilomètres*; Rapport proviso ire; République du Niger, Ministère des Transports et de l'Équipement: Niamey, Niger, 2024.
30. Shrestha, B.B.; Okazumi, T.; Miyamoto, M.; Sawano, H. Flood damage assessment in the Pampanga river basin of the Philippines. *J. Flood Risk Manag.* **2016**, *9*, 355–369. [CrossRef]
31. Merz, B.; Kreibich, H.; Thieken, A.; Schmidtke, R. Estimation uncertainty of direct monetary flood damage to buildings. *Nat. Hazards Earth Syst. Sci.* **2004**, *4*, 153–163. [CrossRef]
32. Jonkman, S.N.; Bockarjova, M.; Kok, M.; Bernardini, P. Integrated hydrodynamic and economic modelling of flood damage in the Netherlands. *Ecol. Econ.* **2008**, *66*, 77–90. [CrossRef]
33. de Moel, H.; van Alphen, J.; Aerts, J.C.J.H. Flood maps in Europe–methods, availability and use. *Nat. Hazards Earth Syst. Sci.* **2009**, *9*, 289–301. [CrossRef]
34. Tiepolo, M.; Rosso, M.; Massazza, G.; Belcore, E.; Issa, H.; Braccio, S. Flood assessment for risk-informed planning along the Sirba River, Niger. *Sustainability* **2019**, *11*, 4003. [CrossRef]
35. Sayers, P.; Li, Y.; Penning-Rowsell, E.; Shen, F.; Wen, K.; Chen, Y.; Le Quesne, T. *Flood Risk Management. A Strategic Approach 2013*; UNESCO: Paris, France, 2013.
36. Critchley, W.; Siegert, K. *A Manual for the Design and Construction of Water Harvesting Schemes for Plant Production*; Food and Agriculture Organisation of the United Nations: Rome, Italy, 1991. Available online: https://www.fao.org/4/u3160e/u3160e00.htm (accessed on 1 June 2026).
37. Water and Sanitation Program. Le Niger Perd 75 Milliards XOF Chaque Année à Cause D'un Mauvais Assainissement. 2012. Available online: https://documents1.worldbank.org/curated/en/627261468124151217/pdf/684660WSP0ESI00ch00PUBLIC00-brochure.pdf (accessed on 1 November 2025).
38. Dasgupta, P.; Sahay, S.; Prakash, A.; Lutz, A. Cost effective adaptation to flood: Sanitation interventions in the Gandak river basin, India. *Clim. Dev.* **2020**, *12*, 717–729. [CrossRef]
39. Brouwer, R.; Sharmin, D.F.; Elliott, S.; Liu, J.; Khan, M.R. Costs and benefits of improving water and sanitation in slums and non-slum neighborhoods in Dhaka, a fast-growing mega-city. *Ecol. Econ.* **2023**, *207*, 107763. [CrossRef]
40. Abdou, A.; Abdoulahi, S.C.; Tidjani, M.A.; Hassimi, M.S.; Sabra, A.K.A.; Soulé, A.E.; Kaire, M. Économie de la Dégradation des Terres à Tahoua, Niger. Analyse Coût-Bénéfice des Activités de Récupération des Terres (Banquettes, Demi-Lunes et Cordons Pierreux) des Quatre Sites de la Commune Rurale de Badaguichiri. 2019. Available online: https://spn2a.org/wp-content/uploads/2020/05/ELD-NIG_Rapport_Tahoua_2019-11-22-ELD-Niger-report-INRAN-web.pdf (accessed on 1 June 2026).
41. Banque Centrale des États de l'Afrique de l'Ouest. Taux D'intérêt Légal 2025 des Pays de L'UMOA. 2025. Available online: https://www.bceao.int/fr/documents/taux-dinteret-legal (accessed on 1 November 2025).
42. Horritt, M.S.; Bates, P.D. Evaluation of 1D and 2D numerical models for predicting river flood inundation. *J. Hydrol.* **2002**, *268*, 87–99. [CrossRef]